HIGH SPIN Mn MOLECULAR CLUSTERS: SPIN STATE EFFECTS ON THE OUTER CORE-LEVEL MULTIPLET STRUCTURES

A. J. NELSON[*], J. G. REYNOLDS[*] and GEORGE CHRISTOU[**]
[*]Lawrence Livermore National Laboratory, Livermore, CA 94550
[**]Indiana University, Department of Chemistry, Bloomington, IN 47405

ABSTRACT

Oxo-bridged manganese polynuclear complexes have applications in a variety of technologies, such as single-molecule nanomagnets, catalysis and photosynthetic redox chemistry. The reason that these types of compounds are capable of such important and varied technologies is thought to be because they possess ground states with large spin values. However, the electronic, structural and magnetochemical relationships are not well understood and need to be thoroughly investigated to adequately explain why Mn is such an integral part of so many useful processes. X-ray photoemission spectroscopy was used to study the Mn 3p, 3s and valence band electronic behavior as a function of Mn cluster structural properties, where the cluster size and nuclearity are systematically varied. Results show a chemical shift of the Mn $3p_{3/2,1/2}$ spin-orbit pair related to the cluster size and nuclearity. Also, the Mn 3s ^7S and ^5S final state multiplet components shift since they involve the binding energy of a ligand valence electron. In addition, the branching ratio of the ^7S:^5S states is related to the 3s–3d electron correlation. Specifically, in the ^7S state, the remaining 3s electron is well correlated with 3d electrons of parallel spin, while in the ^5S state the two spins are antiparallel. Changes in this electron correlation are clearly observed in the ^7S:^5S branching ratio as a function of cluster size and ligand electronegativity.

INTRODUCTION

The multiple oxidation states of transition metal ions make them ideally suited for multielectron processes. Clusters of transition metal ions have been found at the active sites of numerous electron transfer enzymes, notably the tetramanganese cluster in the oxygen evolving complex, the site of water oxidation in photosynthetic organisms.[1] Also, Mn=O, where the oxidation state of Mn is +4 or +5, has been identified as the reactive species in catalytic oxidations with Mn porphyrins.[2,3] These catalytic reactions usually end with the complete conversion of the Mn to permanganate, Mn(VII).[4]

Oxo-bridged manganese polynuclear complexes have also proved useful in the development of single-molecule nanomagnets. [5,6] These molecules have a large ground state spin, S, and a large magnetic hysteresis comparable to that observed in hard magnets. This provides the possibility of molecular bistability, opening the way to store information at the molecular level.

Spin state effects can be examined by x-ray photoemission spectroscopy of outer core-level multiplet structures. Previous photoemission studies on transition metal compounds reveal core-level multiplet structures that are best understood in terms of configuration-interaction (CI) calculations including intrashell electron correlation, charge-transfer and final-state screening.[7-9] In addition, these multiplet structures are also strongly influenced by covalency and ligand coordination.[10,11]

The neutral Mn atom has a $1s^2 2s^2 2p^6 3s^2 3p^6 3d^6$ configuration and a high-spin $[3d^5 4s^2]$ configuration. In solids the (empty) 4s band lies 2 to 4 eV above the top of the $3d^N$ band, depending on the ion. Photoelectron transitions are allowed between the initial state $2p^6 3s^2 3p^6 3d^N$ (N = 3,4,5 for Mn^{+4}, Mn^{+3}, Mn^{+2}, respectively) and a series of final states ($2p^5 3d^{N+1}$).

It has been shown that for Mn dihalides, the outer Mn 3s core-level final state configuration can be either $\underline{3s}3d^5$ or $\underline{3s}3d^6\underline{L}$ depending on final state screening effects due to the ligand ($\underline{3s}$ and $\underline{L}$ indicate that there is one electron missing in the Mn 3s and the ligand valence state, respectively). Also, the 3s final state has ^7S and ^5S symmetry, e.g. the Mn^{2+} initial state $(3s^23p^63d^5)^6S$ has two possible final states, $(3s^13p^63d^5)^7S$ or $(3s^13p^63d^5)^5S$. In the ^7S state, the remaining 3s electron is well correlated with 3d electrons of parallel spin, while in the ^5S state the two spins are antiparallel. This electron correlation reduces the branching ratio of the ^7S:^5S states. In addition, as the ligand electronegativity decreases, charge-transfer satellites become important and the spin state purity is lost in the 3s spectra. The spectra become representative of mixed unscreened ($3d^N$) and locally screened ($3d^{N+1}$) final states. Thus, we see that the 3s core-level is polarized by the $3d^5$ shell.

This paper presents the results of a systematic study of the 3s and 3p core-level photoemission, and satellite structures for Mn oxo-bridged compounds. Outer core-level multiplet splitting was characterized as a function of Mn cluster size, nuclearity and ligand type. Interpretation of the 3p and 3s spectra is consistent with the configuration-interaction (CI) model including intrashell electron correlation, charge-transfer, and final-state screening.

EXPERIMENTAL

The manganese polynuclear complexes are characterized as having trapped-valence oxidation-state Mn cores bridged to various ligands. The Mn cores analyzed are Mn^{3+}, $[Mn_3O]^{6+}$, $[Mn_4O_3]^{7+}$, $[Mn_4O_2]^{8+}$, and $[Mn_{12}O_{12}]^{16+}$. The ligands are dibenzoylmethane (dbm), 2-hydroxymethyl pyridine (hmp), picolinic acid (pic), pyridine (py), and 2-hydroxy-2,4,6-cycloheptatrienone (tropolone or TROP). Note that the ligands dbm, hmp and pic usually bind as anions while pyridine usually forms a neutral complex. The cation tetra-n-butylammonium (TBA) is used as a counter ion. These structures have high ground state spins as determined by the oxidation state and topology of the polynuclear transition metal core.[12-14]

ESCA experiments were performed on a Physical Electronics 5400 ESCA system using Mg Kα radiation (1253.6 eV) and a hemispherical analyzer pass energy of 17.90 eV, giving an overall energy resolution of 1.1 eV. All binding energies are referenced to the Fermi level of the analytical instrument as calibrated to the Au 4f peaks. Binding energies were further referenced to the C 1s photoelectron line arising from adventitious carbon at 284.6 eV to account for charging effects.

RESULTS AND DISCUSSION

Figure 1 shows the Mn 3s and 3p spectral regions for the manganese polynuclear complexes. As previously stated, the excitation energy was 1253.6 eV, and thus the positions and relative intensities of the Mn 3s and Mn 3p multiplets can be considered to be in the sudden limit approximation [7,8] with little coupling between the ion and the photoelectron. The figure shows a chemical shift of the Mn $3p_{3/2,1/2}$ spin-orbit pair associated with the trapped-valence oxidation states. The unresolved 3p peaks are somewhat broadened, but a direct correspondence can be made between observed features in these spectra and those in the literature.[9] Specifically, the main 3p line represents the ^7P ionic final state and the higher binding energy shoulder represents the spin-orbit component $^5P(1)$. Final state screening effects in the core level spectra depend strongly on the electronegativity of the anions (dbm^-, hmp^-, and pic^-) and will affect the final state branching ratio. Specifically, note the variation of the quintet:septet (^7P:^5P) final state branching ratio as the Mn core size increases and becomes a $[Mn_{12}O_{12}]^{16+}$ $Mn^{II}Mn^{III}Mn^{IV}$ trapped-valence oxidation-state. In addition, the covalency of the larger complexes increases manifesting itself as a drastically reduced 3p branching ratio.

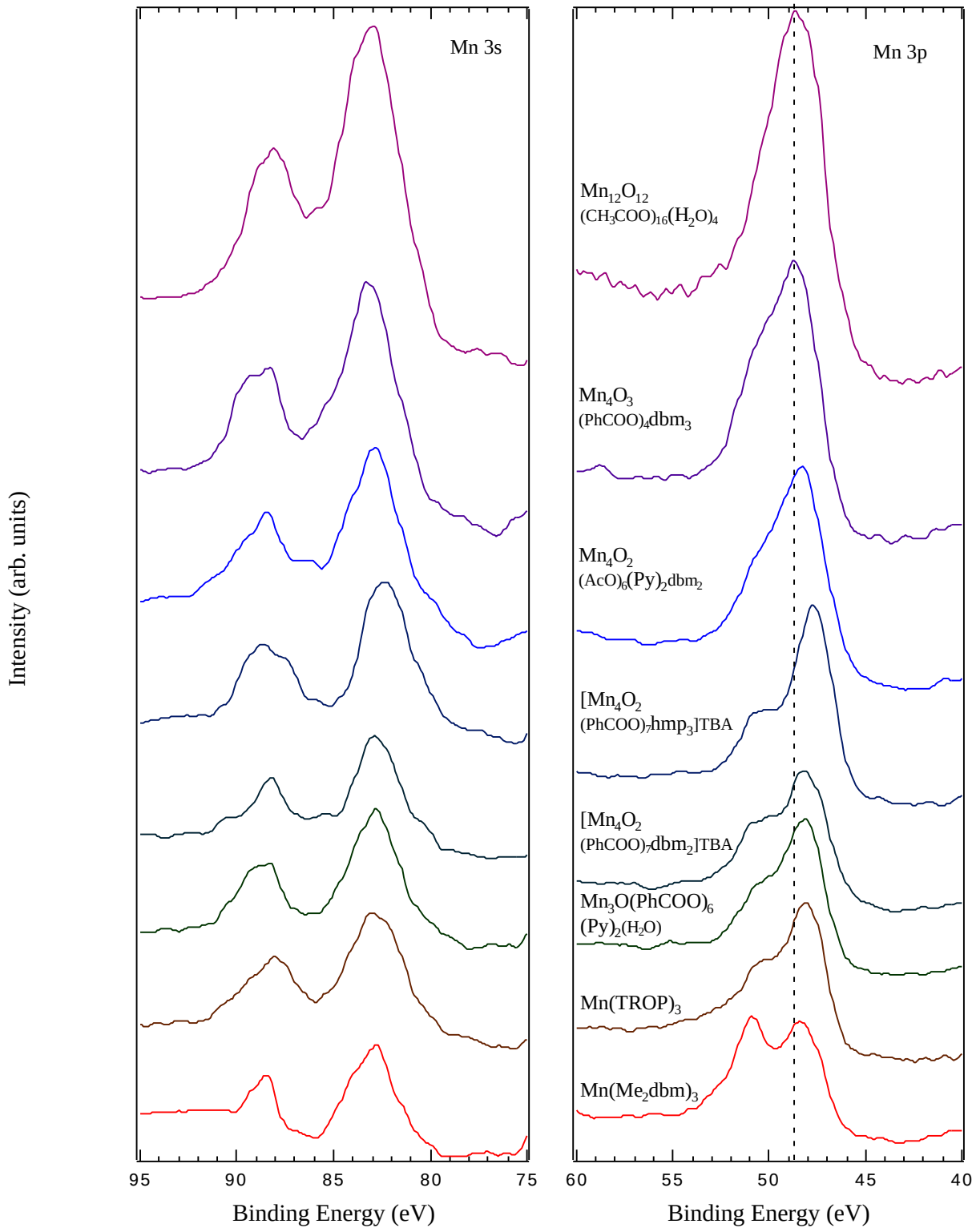

Figure 1. High-resolution XPS spectra of Mn 3p and 3s core levels for the Mn polynuclear complexes.

Table I. Summary of the Mn 3p and 3s Photoelectron Results for Manganese Polynuclear Complexes.

Sample [Mn oxidation state]	Mn 3p (eV)		Mn 3s (eV)		FWHM[a]		ΔMn 3s (eV)	Mn 3s Branching Ratio[b]
	^7P	^5P	^7S	^5S	^7S	^5S		
$Mn(Me_2dbm)_3$ $[Mn^{III}]$	48.4	50.9 Δ=2.5	82.7	88.4	3.0	1.5	5.7	4.4
$Mn(TROP)_3$ $[Mn^{III}]$	48.2	50.2 Δ=2.0	82.7	88.0	3.5	3.2	5.3	1.8
$[Mn_3O(PhCOO)_6$ $(Py)_2(H_2O)]$ $[Mn^{II}, 2Mn^{III}]$	48.2	50.5 Δ=2.3	82.8	88.6	3.2	2.8	5.8	2.2
$[Mn_4O_2(PhCOO)_7dbm_2]$ TBA $[Mn^{III}]$	48.2	50.4 Δ=2.2	82.9	88.2	2.8	2.0	5.3	2.4
$[Mn_4O_2(PhCOO)_7hmp_3]$ TBA $[Mn^{III}]$	47.7	50.2 Δ=2.5	82.4	88.4	3.0	3.2	6.0	1.8
$[Mn_4O_2(AcO)_6$ $(Py)_2dbm_2]$ $[Mn^{III}]$	48.3	50.6 Δ=2.3	82.8	88.4	3.5	3.0	5.6	2.2
$[Mn_4O_3(PhCOO)_4dbm_3]$ $[3Mn^{III}, Mn^{IV}]$	48.7	50.8 Δ=2.1	83.2	88.5	3.2	3.0	5.3	2.1
$[Mn_{12}O_{12}$ $(CH_3COO)_{16}$ $(H_2O)_4]$ $[Mn^{II}, Mn^{III}, Mn^{IV}]$	48.7	–	83.1	88.2	3.8	4.8	5.1	1.4

a) Full width half-maximum of Mn 3s peaks in eV.

b) The branching ratio of the Mn 3s peaks are based the area ratio of the ^7S:^5S states.

The binding energy positions for the Mn 3s ^7S and ^5S multiplet components are summarized in Table I. Note that the Mn 3s multiplet splitting (ΔMn 3s) becomes smaller as the Mn trapped-valence oxidation state increases, consistent with published data.[7-9] Also note that the ^7S and ^5S multiplet components shift accordingly since they are correlated with charge transfer between the Mn *d*-states and ligand *p*-states. In addition, note that the FWHM of the ^5S multiplet component is affected by ligand chemistry consequently affecting the Mn 3s branching ratio. Specifically, as the ligand electronegativity decreases, charge-transfer from the ligand *p*-state to the Mn *d*-state causes the spin state purity to be lost in the 3s spectra. Thus, the branching ratio corresponding to S – 1/2 and S + 1/2 final states that principally reside on the p orbitals of the [ligand]- and the d orbitals of the [MnO]+ core, decreases. Note that the branching ratios for complexes with the dbm ligand are larger since the ^5S component is diminished indicating that the s and d electrons spins are mostly parallel.

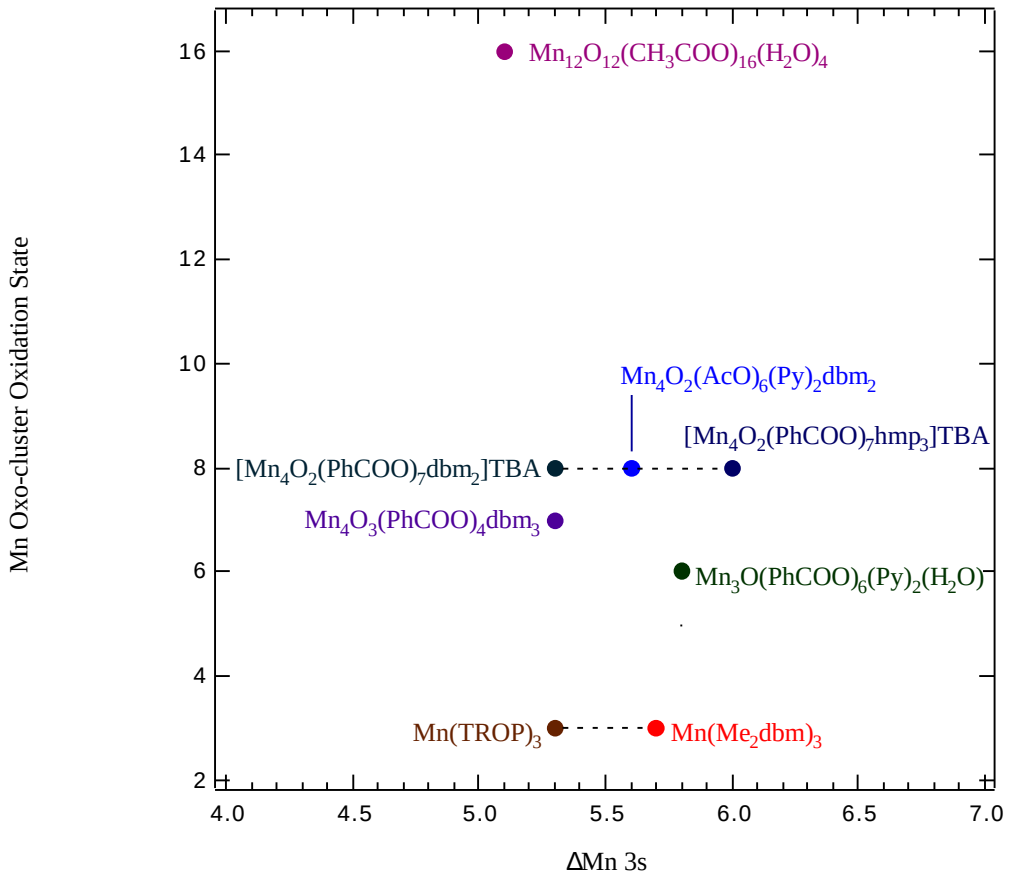

Figure 2. Mn cluster oxidation state versus Mn 3s multiplet splitting for the Mn polynuclear complexes.

Figure 2 graphically summarizes the Mn cluster oxidation state versus Mn 3s multiplet splitting for the Mn polynuclear complexes. The multiplet splitting for these ligands is an indication of the 3s polarization by the 3d final states. Also, polarization of the ligand can delocalize mobile π electrons and thus affect multiplet splitting.

The polynuclear complex with the largest core size and the $[Mn_{12}O_{12}]^{16+}$ $Mn^{II}Mn^{III}Mn^{IV}$ trapped-valence oxidation-state, exhibits the smallest Mn 3s branching ratio. However, this can be affected by the electronic properties of the ligand. Specifically, note that the variation of the Mn 3s multiplet splitting for the three complexes with the $[Mn_4O_2]^{8+}$ cores is due to the different ligand electronegativities, the dbm ligand having a higher electronegativity than the hmp ligand. Similarly for the two complexes with Mn^{3+} cores, the TROP ligand having a higher electronegativity than the Me_2dbm ligand.

CONCLUSIONS

We have presented the results of a systematic study of the 3s and 3p outer core-level multiplet splitting as a function of Mn cluster size, nuclearity, and ligand type. Results show that the Mn 3p final state branching ratio changes as the Mn core size and trapped-valence oxidation-state increases. In addition, as the covalency of the larger complexes increases the 3p branching ratio is reduced. Results also show that the Mn 3s multiplet splitting became smaller as the Mn trapped-valence oxidation state increased. The observed multiplet splitting provides further understanding of these oxo-bridged manganese polynuclear complexes.

Acknowledgments

This work was performed under the auspices of the U.S. Department of Energy by University of California, Lawrence Livermore National Laboratory under contract No. W-7405-ENG-48.

REFERENCES

1. V.K. Yachandra, K. Sauer, and M.P. Klein, Chem. Rev. **96**, 2927 (1996).
2. J.T. Groves and M.K. Stern, J. Am. Chem. Soc. **110**, 8628 (1988).
3. J.T. Groves, J. Lee, and S.S. Marla, J. Am. Chem. Soc. **119**, 6269 (1997).
4. J. Limburg, G.W. Brudvig, and R.H. Crabtree, J. Am. Chem. Soc. **119**, 2761 (1997).
5. D. Ruiz-Molina, G. Christou, D.N. Hendrickson, Mol. Cryst. Liq. Cryst. **343**, 335 (2000).
6. J. Yoo, E.K. Brechin, A. Yamaguchi, M. Nakano, J.C. Huffman, A.L. Maniero, L.C. Brunel, K. Awaga, H. Ishimoto, G. Christou, and D.N. Hendrickson, Inorg. Chem. **39**, 3615 (2000).
7. P.S. Bagus, A.J. Freeman and F. Sasaki, Phys. Rev. Lett. **30**, 850 (1973).
8. C.S. Fadley, in *Electron Spectroscopy: Theory, Techniques, and Applications,* edited by C.R. Brundle and A.D. Baker (Academic, London, 1978) Vol. II, Chap. 1.
9. B. Hermsmeier, C.S. Fadley, B. Sinkovic, M.O. Krause, J. Jimenez-Mier, P. Gerard, T.A. Carlson, S.T. Manson and S.K. Bhattacharya, Phys. Rev. **B48**, 12425 (1993).
10. M. Fujiwara, T. Matsushita and S. Ikeda, J. Electron Spectroscopy Rel. Phenom. **74**, 201 (1995).
11. A. J. Nelson, J. G. Reynolds and J. W. Roos, J. Vac. Sci. Technol. **A18(4)**, 1072 (2000).
12. Michael W. Wemple, H.-L. Tsai, S. Wang, Juan Pablo Cluade, W.E. Streib, J.C. Huffman, D.N. Hendrikson and George Christou, Inorg. Chem. **35**, 6437 (1996).
13. S. Wang, H.-L. Tsai, Eduardo Libby, K. Folting, W.E. Streib, D.N. Hendrikson and George Christou, Inorg. Chem. **35**, 7578 (1996).
14. Sheyi Wang, Michael S. Wemple, Jae Yoo, Kirsten Folting, John C. Huffman, Karl S. Hagen, David N. Hendrickson, and George Christou, Inorg. Chem. **39**, 1501 (2000).